Journal of Power Sources 394 (2018) 26–34

Contents lists available at ScienceDirect

Journal of Power Sources

journal homepage: www.elsevier.com/locate/jpowsour

A hybridized solid-gel nonflammable Li-Battery

Guibin Li[a], Xin Chen[a], Lixiao Miao[b], Jitao Chen[a], Junrong Zheng[a,*]

[a] College of Chemistry and Molecular Engineering, Peking University, Beijing 100871, China
[b] National Center for Nanoscience and Technology, Chinese Academy of Sciences, Beijing 100190, China

HIGHLIGHTS

- Bi-functional rigid-flexible non-wovens-based polymer electrolytes.
- Excellent thermal stability, mechanical properties, high ion conductivity.
- No shrinkage under open flame, no volumetric expansion at high temperature.
- Excellent electrochemical performances with suppression of lithium dendrite growth.

GRAPHICAL ABSTRACT

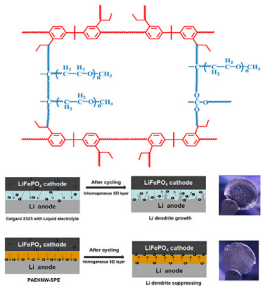

ARTICLE INFO

Keywords:
Poly (aryl ether ketone) non-woven fabric
3D cross-linking network
Solid polymer electrolyte
Safety reinforced
Lithium metal battery

ABSTRACT

Most Li-metal batteries can work safely only under 45 °C and have risks of burning or explosion. A novel non-flammable Li-battery is developed to address the challenge, using an interpenetrating rigid-flexible poly (aryl-ether-ketone) nonwovens (PAEKNW) cross-linked with poly(ethylene glycol) dimethacrylate electrolyte to transport lithium ions. The hybridized polymer electrolyte possesses a high ionic conductivity of 1.2×10^{-3} S cm^{-1} at room temperature and a wide electrochemical window with decomposition voltage higher than 4.5V. It does not readily catch fire or shrink, even under open flame, and shows no noticeable volumetric expansion or contraction at 80 °C, in stark contrast to most liquid-electrolytes-based or gel batteries. Even after cut off by one-third, the battery continues to function. The unique bi-functional molecular design of the polymer electrolyte, which guarantees simultaneously a very rare combination of thermal and mechanical stability, high ion conductivity, and a wide electrochemical window at room temperature, is the key factor responsible for the excellent comprehensive performances.

1. Introduction

In recent years, rechargeable lithium-ion batteries have gained extensive applications in consumable electronic devices, automobiles, and energy storage [1–4]. Meanwhile, the demand for larger storage capacity and higher power density is increasing rapidly along with the need for more powerful portable electronic devices and large-scale energy storage systems [5–9]. However, more powerful batteries are often accompanied with greater risks of burning or even explosion. li-batteries in electric cars or cell phones catching fire or exploding become less uncommon in these days [10,11]. The temperature safety limit of most Li-batteries used in automobiles nowadays is only about 45 °C, mainly because of the flammable volatile electrolyte solvent used in those batteries, which severely limits the application in many places, particularly during the summer time.

It has been proposed that solid polymer electrolytes (SPE) combined with Li metal anode can be the potential solution [12–14]. Li metal, with the highest theoretical capacity of 3860 mA h g^{-1}, can serve as an

* Corresponding author.
E-mail address: junrong@pku.edu.cn (J. Zheng).

https://doi.org/10.1016/j.jpowsour.2018.05.048
Received 13 February 2018; Received in revised form 24 April 2018; Accepted 12 May 2018
Available online 15 May 2018
0378-7753/

ideal anode material [15–17]. Unfortunately, lithium metal is thermodynamically unstable in liquid electrolytes, and lithium dendrites grow during charge/discharge cycles and usually cracks as a result of volumetric expansion, eventually leading to short circuit, thermal runaway, and other serious safety issues [18,19]. Replacing the flammable liquid carbonate electrolytes with SPEs can mitigate or even prevent the growth of dendrite nucleation and therefore significantly improve the safety performance [20–22]. Among many polymeric systems tested as SPE, poly(ethylene oxide) (PEO)-based polymers are most widely used and their advantages have been recognized [23–27]. However, its relative low ionic conductivity at room temperature [28–30], narrow electrochemical stability window (4.2V vs Li^+/Li) and high working temperature (typically > 60 °C) [31,32] hinder their applications, particularly in high-energy solid Li-metal batteries. Many other polymers have also been reported for this application, such as poly(ethylene glycol acrylate) and other amorphous polymers [33–35]. Despite of improved ionic conductivities, most of these flexible polymeric materials have inferior mechanical strength, e.g. shrink once heated, and cannot suppress the lithium dendrites growth because of their poor interfacial adhesion with the Li anode [36]. Battery cells made with these soft SPE, as well as most gel polymer electrolytes, often suffer from the risks of short circuit or even combustion.

An ideal Li-battery electrolyte system should simultaneously have high thermal and mechanical stability, high ion conductivity and a wide electrochemical window at room temperature. However, some of these properties seem to contradict with each other, e.g. high thermal and mechanical stability vs high ion conductivity, in most polymer systems. In this work, we are able to overcome this barrier, by developing a novel bi-functional polymeric electrolyte system that possesses all these desirable features. Li-Batteries fabricated with this new material exhibit exceptional safety properties, e.g. do not catch fire over open flame, do not shrink or expand under elevated temperature, and work normally even when physically damaged.

2. Experimental section

2.1. Materials

Diallyl Bisphenol A (DBA), 2,2-bis(4-hydroxyphenyl) propane (BP), Dimethyl sulfoxide (DMSO), poly(ethylene glycol) dimethacrylate (PEGDMA, average Mn = 900), 2-Hydroxy-2-methylpropiophenone (photo-initiator) and 4,4′-Difluorodiphenyl methanone (DFDP) are purchased from Aladdin. Liquid electrolyte of 1 M LiPF6 in EC/DMC/DEC (1:1:1 by volume) with 4% fluoroethylene carbonate (FEC) and lithium tablets are purchased from Beijing Institute of Chemical Reagents. Ethyl alcohol absolute, ethoxylated trimethylolpropane triacrylate (ETPTA), N,N-Dimethyl formamide (DMF), toluene and potassium carbonate are purchased from Sigma-Aldrich. The battery membranes are purchased from K.J. Group, including the celgard 2325 and 25 μm micro porous trilayer membrane (PP/PE/PP). All solvents and reagents are reagent grade and used as received.

2.2. Synthesis of PAEK polymers and preparation of nonwoven fabric

The synthetic procedure of poly (aryl ether ketone) (PAEK) with propylene group is shown in Scheme 1. Samples of DBA (4.60 g,12 mmol), BPA(3.42 g, 28 mmol), DFDP (7.63 g, 40 mmol), K_2CO_3 (4.56 g, 44 mmol), DMSO (52 ml) and toluene (24 mL) are added into a 250 ml three-neck flask equipped with a mechanical stirrer, a dean stark trap, and a nitrogen inlet/outlet. The solution is allowed to reflux at 140 °C, and water is azeotropically removed from the reaction mixture. After 4 h, the toluene is removed from the reaction by slowly increasing the temperature to 170 °C, and then the reaction is allowed to continue for another 2–3 h. When the viscosity is observed to increase dramatically, the mixture is slowly poured into 1000 ml deionized water. The resulted fibrous copolymer is washed with hot water several times and dried under vacuum at 80 °C for 24 h to obtain the modified PAEK. ^{1}H NMR (400 MHz, $CDCl_3$, TMS): δ 1.71 (s, 78 H), 5.71–5.75 (m, 2H), 6.19–6.25 (m, 4H), 6.37 (d, 3H, J = 11.2 Hz), 6.50 (d, 3H, J = 15.6 Hz), 7.01 (dd, 82H, J = 8.8, 11.6 Hz), 7.24 (t, 28 H, J = 4.4 Hz), 7.78 (d, 44H, J = 8.4 Hz); ^{13}C NMR (100 MHz, $CDCl_3$): δ 31.0, 42.4, 117.1, 119.6, 128.3, 132.2, 146.7, 153.5, 161.4, 194.3.

The preparation of a porous PAEK nonwoven is conducted with electrostatic spinning equipment. 2g of PAEK polymer is dissolved in 18 ml of DMF to obtain a solution with a weight ratio of 10%. The mixed copolymer solution is sucked into the syringe, and then ejected. The ejection rate and the rotation speed of the receiver are adjusted to obtain the optimal condition. The loading voltage is set at 15 kV. The obtained white porous nonwoven fabric (10 cm × 20 cm) membranes are then dried in vacuum at 100 °C for 12 h to remove remaining solvent and roll-pressed under 10 M Pa. The liquid uptake and porosity are calculated according to literature [46].

2.3. The preparation of UV-curing PAEKNW-based solid polymer electrolyte (PAEKNW-SPE)

Using lithium tablet as substrate, a homogeneous solution of PEGDMA, liquid electrolyte, ETPTA, and 2,2-bis(4-hydroxyphenyl) propane (BP, photoinitiator) are first mixed with a ratio of 1:2.5:0.1:0.01 and then injected into PAEKNW which has been placed on the surface of Li foil. The polymer electrolyte/Li anode assembly is fabricated in situ after exposed to UV irradiation for 5 min. The thickness of the PAEKNW-based solid polymer electrolyte (PAEKNW-SPE) is about 70 microns.

2.4. Characterization

^{1}H NMR measurements are conducted with a 400 MHz Bruker Avance using $CDCl_3$ as solvent and tetramethylsilane (TMS) as the standard. The morphologies of PAEKNW membrane, PAEKNW-SPE and the Li anode after cycling are characterized by field-emission scanning electron microscope (SEM). TGA measurements of all membranes are performed using a Perkin-Elmer TGA-1 thermo-gravimetric analyzer with a heating rate of 10 °C min^{-1} under nitrogen atmosphere. FT-IR spectra of dry membrane samples are recorded on the power samples dispersed in dry KBr, using a BRUKER Vector 22 Fourier-transform infrared spectrometer with a resolution of 4 cm^{-1}. The mechanical properties of the dry membranes are measured at room temperature on SHIMADZU AG-I 1 KN with a strain rate of 2 mm/min. At least five samples (15 mm × 4 mm) are used for each measurement and their average values are calculated.

The electrochemical stability window is examined using an Autolab PGSTAT100 electrochemical workstation, with linear sweep voltammetry performed on a working electrode of platinum plate and a counter and reference electrode of PAEKNW- SPE modified Li metal with a scan rate of 1 mV s^{-1} at room temperature.

The temperature dependence of ionic conductivity is determined by impedance spectroscopy measurements, using the same electrochemical work-station within a temperature range of 20 °C–80 °C. Briefly, 10 mV is applied to two stainless steel electrode cells, which are loaded with the PAEKNW-GPE in a frequency range from 100 kHz to 10 Hz. The ionic conductivity is calculated by the following equation:

$$\sigma = \frac{L}{RS} \quad (1)$$

where σ is the proton conductivity (S cm^{-1}), L is the distance between the two electrodes, R is the resistance value of the membrane and S is the cross section area of the membrane (cm^2).

Porosity and liquid uptake of the membranes are determined by the *n*-butanol adsorption method according to literature [47]. After immersing the membrane in *n*-butanol for 2 h, the membranes are weighed before and after adsorption of *n*-butanol, and calculated

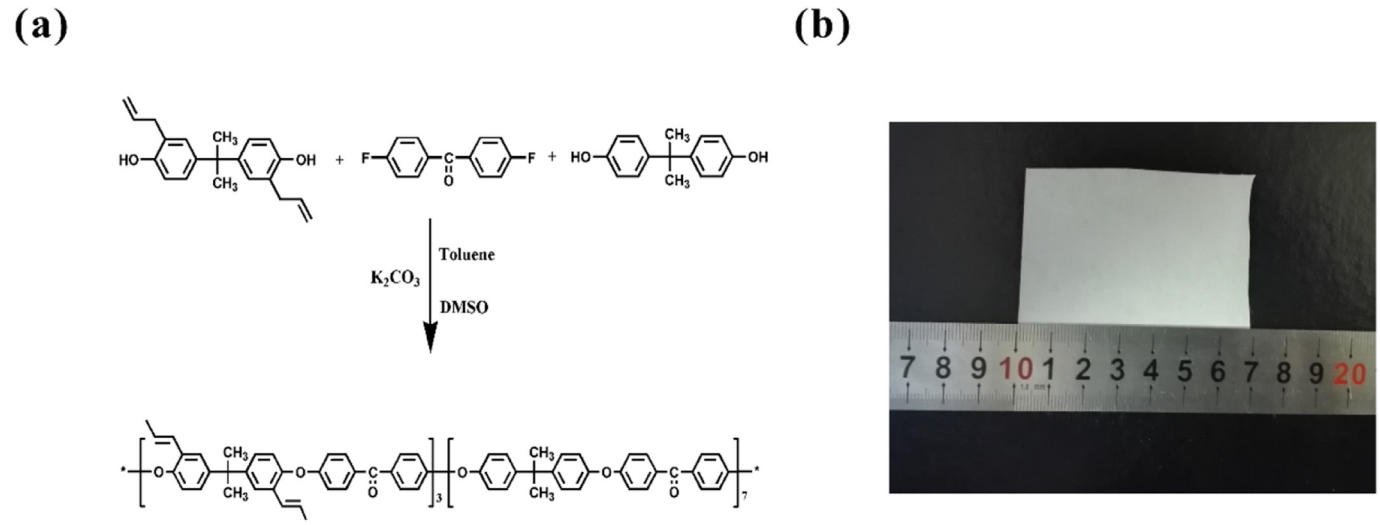

Scheme 1. (a) The preparation of PAEK with 30% of repeating unit modified with propylene group; (b) a sample of PAEKNW.

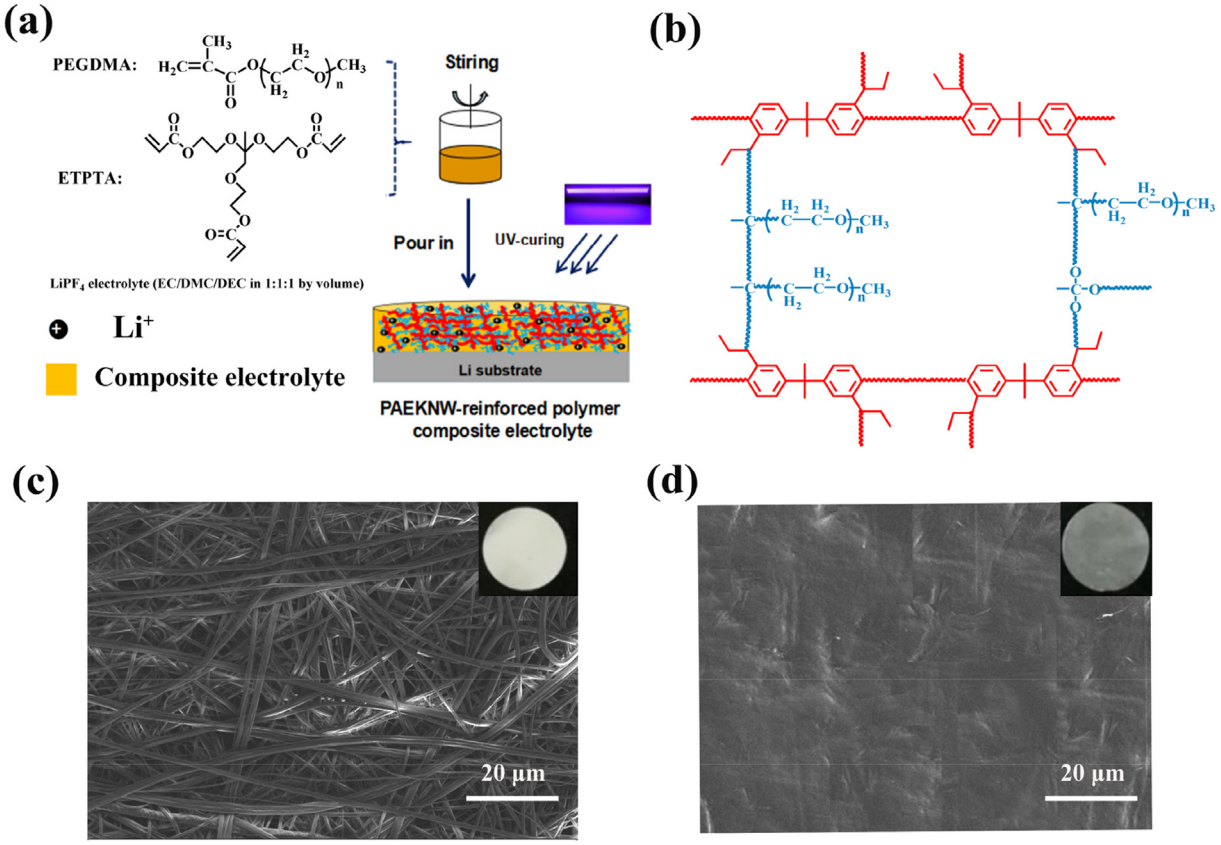

Fig. 1. (a) Preparation procedure of the nonflammable electrolyte system. (b) Molecular structure of the 3D interpenetrating polymer network. (c) SEM and optical (insert) images of the polymer backbone NWF. (d) SEM and optical (insert) images of the electrolyte film after UV-curing.

according to the following equations:

$$Porosity = \frac{(m1 - m2) \times \rho p}{(m1 - m2)\rho p + m2\rho n} \quad (2)$$

$$and\ \ Liquid\ \ uptake = \frac{m1 - m2}{m2} \times 100\%, \quad (3)$$

where the m_1 and m_2 are the weights of the wet and dry membranes, respectively, and $\rho n$and $\rho p$are the densities of *n*-butanol and PAEK, respectively.

Li cycling efficiency is measured in a Li/Cu cell with a LANHE CT2001A battery tester. A certain amount of Li is Galvanostatically plated onto the Cu substrate under the condition of 0.3 mA for 2 h. The plated Li is galvanostatically stripped out of the Cu substrate at 0.3 mA until the voltage reaches 1V. The specific value of stripping/plating time is calculated accordingly and the coulombic efficiency is obtained.

2.5. Cathode preparation and testing of lithium metal cells

The cathode slurry is prepared by mixing $LiFePO_4$ powder, Super P carbon black, and PVDF (polyvinylidene difluoride) with a 90:5:5 wt

ratio in N-methylpyrrolidone (NMP). The aluminum foil is coated with the viscous slurry using a film-casting doctor blade. The obtained electrode films with an active material $LiFePO_4$ loading of around 5 mg cm^{-2} is dried at 90 °C for 12 h in a vacuum oven for fabricating coin cells before using them to assemble the coin cells. Charge–discharge tests are carried out over a voltage range of 2.65–3.85 V at room temperature (25 °C) with a cell test instrument after the cells are allowed to age for 6 h. The current is determined using the theoretical capacity of 170 mA h g^{-1} for the Li/$LiFePO_4$ cell. Cells are galvanostatically cycled with a LANHE CT2001A battery tester.

3. Results and discussion

3.1. Fabrication and morphology of UV-curing PAEKNW-SPE

The backbone of the electrolyte is a derivative of engineering plastic, poly (arylene ether ketone) (PAEK) which has exceptional thermal and mechanical stability [37–39]. This polymer has propylene groups on its side-chains as covalent-bond linkers to electrolyte. It is fabricated into porous non-woven fabrics (NWF) structures with an electrostatic spinning technology. A soft poly (ethylene glycol) dimethacrylate (PEGDMA) polymer containing $LiPF_6$ solution is attached to the propylene groups by UV-curing polymerization. The preparation procedure of the electrolyte system is illustrated in Fig. 1a, and the bi-functional polymer structure is displayed in Fig. 1b. The process results in a rigid-flexible 3D interpenetrating polymer network (PAEKNW-SPE), in which the thermally stable backbone and the ion-conducting flexible filler are linked by covalent bonds, preventing phase separation between them.

The SEM and optical images of the rigid backbone NWF and the electrolyte film are displayed in Fig. 1c&d. The rigid backbone PAEKNW membrane is a piece of white fabrics, consisting of irregularly aligned polymer microfibers, with average diameter around 1 ~ 2 μm. The gaps among the microfibers are typically larger than 3 μm (Fig. 1c). Once cross-linked with the polymer PEGDMA electrolyte, the gaps are filled and the surface of the membrane becomes much smoother and more homogenous (Fig. 1d).

3.2. Characterization of polymers and PAEKNW

The structure of PAEK is confirmed by ^1H NMR measurements in $CDCl_3$ as shown in Fig. S1. According to results in literature [37], the allyl group in the molecular structure resonates with propylene in alkaline conditions. In the ^1H spectrum, a peak between 6.6 ppm and 6.3 ppm corresponds to the hydrogen atom of propylene group. In addition, the characteristic peaks of the remaining hydrogen atoms in the PAEK molecular structure correspond to the results of the standard spectrum perfectly, and this confirms that the PAEK modified with propylene groups has been successfully prepared.

The UV-initiated polymerization of PAEKNW and PEGDMA are identified by FTIR spectroscopy and the result is shown in Fig. S3. The peak corresponding to the C = C propylene of PAEK at 900 cm^{-1} does not appear in the spectrum after the UV-curing, whereas other peaks of PAEKNW and UV-curing product of PAEKNW with PEGDMA are almost the same, which confirms that propylene has reacted with the allyl of PEGDMA. The UV-curing reaction of PAEK, PEGDMA with ETPTA was shown in Fig. S2.

3.3. Fire resistance and thermal stability

This polymer electrolyte has amazing fire resistance and thermal stability. As shown in the left panel of Fig. 2a, it does not catch fire, even under open flame. Furthermore, no apparent deformation or shrinkage can be observed after exposed in open flame for 2 min (central panel of Fig. 2a). This ability to retain shape is a key factor to prevent the cathode and anode of Li-battery from short-circuit under elevated temperature. In stark contrast, a commercial polypropylene membrane, Celgard 2325, undergoing the same tests readily catch fire and shrink for more than 80% (left and central panels of Fig. 2b).

The exceptional thermal stability of PAEKNW-SPE can be rationalized by molecular design. The backbone PAEK polymer itself is well known for its excellent fire resistance. Its repeated rigid benzene rings guarantee very high melting point (> 340 °C) and glass transition temperature (> 150 °C). Under 440 °C, its weight loss is less than 5%. These properties provide the polymer framework excellent resistance to combustion or deformation at high temperature. We also compare the melting point T_m, porosity and liquid uptake of PAEKNW-SPE with those of celgard 2325 in, as shown in Table S1. Due to the NW-fabric porous structure, the porosity and liquid uptake of PAEKNW reach 73% and 240%, respectively, which are higher than those of Celgard 2325. The special rigid molecular structure provides PAEK excellent thermal stability and a higher melting point (T_m > 300 °C). PAEKNW can maintain structure-stability at higher temperature compared with Celgard 2325. Its glass transition temperature (T_g) and $T_{5\%}$ reach 150 °C and 432 °C, respectively, as shown in Fig. S4. Although the soft filler PEGDMA which uptakes about 50% liquid electrolyte has low melting and glass transition temperatures and is easy to deform at high temperature, it does not produce noticeable effect on the macroscopic dimensions of electrolyte film probably because it is covalently bonded and confined within the micron-sized cavities of the rigid framework. By itself, the liquid electrolyte is flammable and easy to vaporize. However, the polar liquid molecules have strong intermolecular interactions with the carbonyl and ether groups of the polymer matrix, which provides attraction force to retain them within the polymer matrix even under heated. Commercial membranes made of polypropylene or polyethylene are nonpolar polymers. Their interaction with the polar electrolyte liquids is much weaker and unable to keep the liquids inside the polymer matrix once heated. In addition to the flame tests, high temperature tests on soft package batteries further support this argument. As displayed in the right panel of Fig. 2a, a soft package battery with Li metal as anode, $LiFePO_4$ as cathode, and PAEKNW-SPE as electrolyte, does not swell after heated under 80 °C for 1 h, and the weight loss of PAEKNW-SPE is less than 19% after 2 h, as shown in Fig. S5. On contrast, a battery made of commercial Celgard 2325 film and liquid electrolyte swells for more than 100% under the same test conditions (right panel of Fig. 2b).

3.4. Electrochemical characteristics

In contrast to typical solid polymer electrolytes of which ion conductivity is too low for batteries to function at room temperature [29,30], the bi-functional PAEKNW-SPE has not only excellent thermal stability and mechanical stiffness, but also very high ion conductivity at room temperature. Fig. 3a displays the temperature-dependent ionic conductivity (σ) of PAEKNW-SPE. Its conductivity σ maintains at a high level of about 10^{-3} S cm^{-1} from 20 °C to 70 °C (green), comparable to (about 50% lower than) the commercial liquid electrolyte (black), but orders of magnitude higher than a typical polymer electrolyte (red). The ion conductivity is sufficiently high for batteries to work at room temperature. The temperature dependence of PAEKNW-SPE ion conductivity is very interesting. Although PAEKNW-SPE is a solid sample, it behaves significantly different from a typical solid state polymer PEO electrolyte (Fig. 3a, red) but very similar to the liquid sample (Fig. 3a, black). We believe that this liquid-like ionic behavior is the result of the unique PAEKNW-SPE rigid-flexible molecular structure.

To further study the electrochemical impedances of liquid electrolyte, PAEKNW-SPE and PEO/LiTFSI, the nyquist plots of these cells at different temperatures are shown in Fig. 3c. It's clear that, the PAEKNW-SPE and liquid electrolyte have similar electrochemical impedances which are less than 10 Ω at 20 °C. In stark contrast, the impedance of PEO/LiTFSI is still much higher than PAEKNW-SPE even at

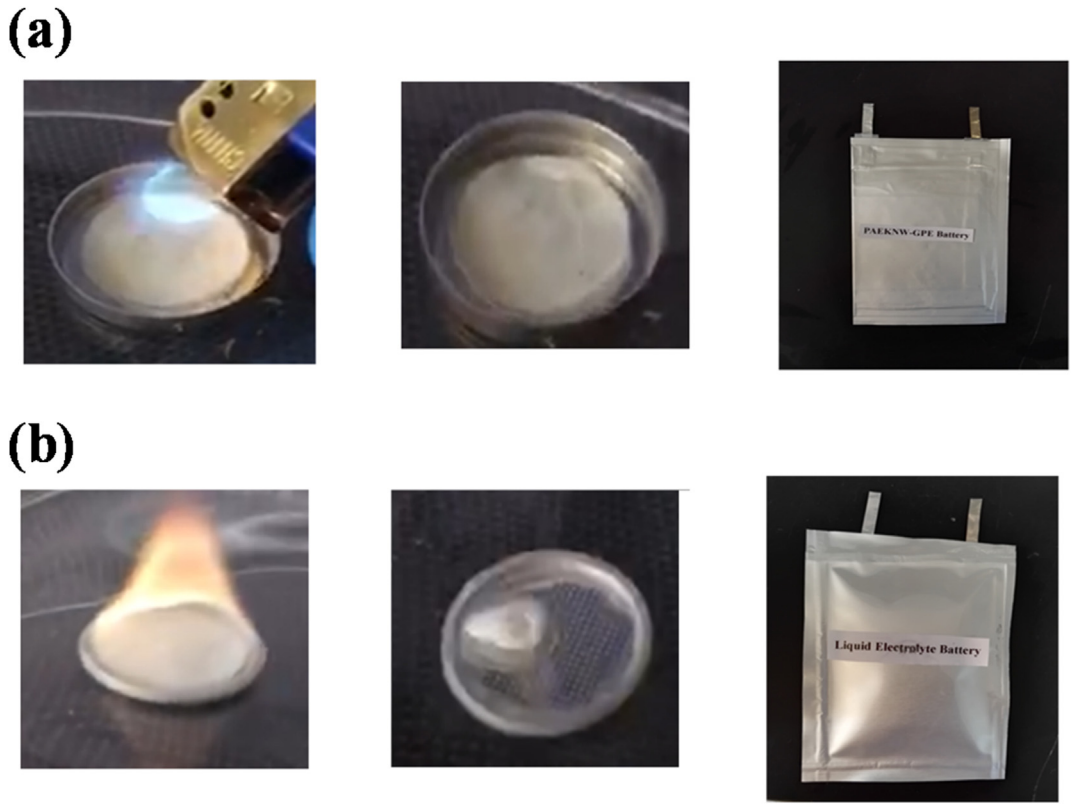

Fig. 2. Comparison between (a) PAEKNW-SPE and (b) commercial PP membrane (Celgard 2325) liquid electrolyte. PAEKNW-SPE doesn't catch fire or deform under open flame. Its soft package battery with Li metal as anode and $LiFePO_4$ as cathode doesn't swell after heated under 80 °C for 1 h. On contrast, Celgard 2325 with liquid electrolyte readily catches fire and shrinks significantly, and its battery swells for more than 100% under the same test conditions.

60 °C or 70 °C. On one hand, the PAEK backbone provides mechanical support. On the other hand, the soft filler PEGDMA provides fast ion conductivity. PEGDMA resembles many polymer gels inside which liquid molecules are trapped by relatively strong intermolecular interactions. The interaction between PEGDMA and carbonate liquid molecules is mostly polar/polar interaction which is similar to those interactions within the liquid itself. The interaction strength is typically smaller than 3 kcal/mol [40], allowing the solvent-bound Li^+ cation to rotate or move within a few picoseconds [41,42]. Such fast kinetics enables fast Li^+ transportation at the molecular level.

PAEKNW-SPE has a very wide electrochemical window. As displayed in Fig. 3b (red), PAEKNW-SPE shows no obvious decomposition below 4.5V versus Li^+/Li, which is notably higher than the typical decomposition voltage threshold of PEO (4.2V). The result seems surprising, because the molecular structure of PEO and the soft filler PEGDMA are essentially the same. Most Li^+ cations are contained in PEGDMA. Under electrochemical oxidation, one would expect the less stable PEGDMA (4.5 versus Li^+/Li) rather than the stable PAEK to decompose first, and the decomposition voltage should be similar to that of its neat polymer (PEO). The fact that PAEKNW-SPE has an obviously larger electrochemical window suggests that the rigid backbone PAEK functions beyond a mechanical support or a fire extinguisher. It is conceivable that its pi-electrons on benzene rings provide extra screening effect to protect PEGDMA from external applied electric field or current.

Another advantage of the rigid-flexible molecular architecture is that it can effectively suppress the growth of Li dendrites on the metal anode, resulting in superior electrochemical stability. As displayed in Fig. 4a&b, Li dendrites immediately grow on the anode in a battery made with the commercial Celgard 2325 film and liquid electrolyte (Fig. 4a) after only 20 charge/discharge cycles. The dendrite growth is significantly slower in the PAEKNW-SPE battery (Fig. 4b). The difference can be easily understood based on crystal growth mechanism. In liquids, Li^+ cations to be reduced have free space to grow sharp branches on the anode (Fig. 4c). This is a kinetic-controlled process. On the interface between the anode and PAEKNW-SPE, however, most Li^+ cations are confined inside the polymer, and very little free space is available for the growth of tree-like Li crystals (Fig. 4d). Instead, thermodynamics (the energy imposed by the polymer framework) force them to grow along the interface. This leads to very different electrochemical stabilities. As displayed in Fig. 4e, in the liquid electrolyte symmetric cell (Li/separator–liquid-electrolyte/Li), the voltage polarization increases sharply with time, and the cell eventually stops working due to short circuit induced by Li dendrites at about two hundred hours. In a sharp contrast, no obvious overpotential increments are observed for 300 h in a Li/PAEKNW-SPE/Li symmetrical cell (Fig. 4f).

3.5. LiFePO4/PAEKNW-SPE/li battery performances

To assemble a full battery, we choose $LiFePO_4$ as the cathode material, Li metal as the anode, and PAEKNW-SPE as the electrolyte. $LiFePO_4$ is a very stable compound which has been extensively used in automobile batteries. In the battery, all the three components are solids, and PAEKNW-SPE is the least stable one. Therefore, the safety performances of the battery are mainly determined by PAEKNW-SPE. As discussed above, owing to PAEKNW-SPE's exceptional mechanical and thermal stability, the battery can work safely at temperature as high as 80 °C, with no risks of combustion. In addition, because PAEKNW-SPE is a solid sample, the battery can still function normally even when physically damaged. As displayed in Fig. 5, the battery works normally after punctured all the way through with a nail (Fig. 5b), or one-third cut off (Fig. 5c). No shorted circuit or leakage of electrolyte occurs during these harsh tests. Only a very small voltage drop (less than

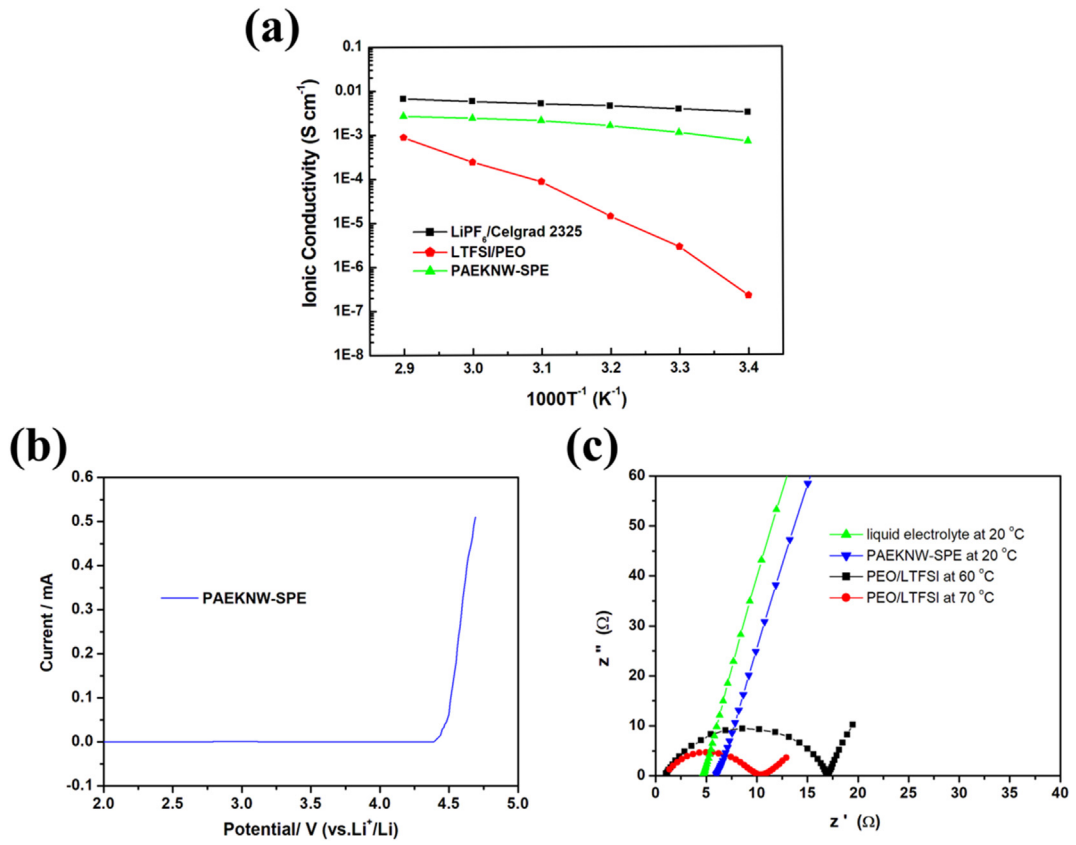

Fig. 3. (a) Ionic conductivities of liquid electrolyte, PAEKNW-SPE and PEO solid state polymer electrolyte at temperatures from 20 °C to 70 °C. (b) Linear sweep voltammetry of the PAEKNW-SPE in platinum sheet cells at room temperature. (c) Electrochemical impedance spectra of liquid electrolyte, PAEKNW-SPE and PEO/LiTFSI at different temperatures.

0.04V) is observed after one third is cut off.

The safety performances of the PAEKNW-SPE battery are similar to those solid state polymer batteries [17,43]. However, different from those solid state counterparts that can only work at elevated temperature, the PAEKNW-SPE battery works very well at room temperature because of PAEKNW-SPE's liquid-like ion conductivity. As shown in Fig. 6a, at room temperature, the specific capacity of the battery reaches as high as 146 mAh g^{-1} and 72 mAh g^{-1} at 0.1C and 5C, respectively. The polarization potential shows little rate-dependence, as evident in the charge/discharge curves of first cycle under different rates in Fig. 6b. We also assemble Li/Cu cells to study the coulombic efficiency of Li plating/stripping. As shown in Fig. 6c, after discharging for 2 h at a constant current of 0.3 mA, the cell takes about 1.82 h to reach the cut-off voltage (1V) at 0.3 mA. The stripping/plating ratio is higher than 90%, which is beneficial for the cycling stability. After 200 cycles at a rate of 0.5C, the capacity remains at 124 mAh g^{-1}, nearly 92% of its initial capacity (Fig. 6d). At a higher charge/discharge rate of 1C, as depicted in Fig. 6e, after 200 cycles the capacity decreases slightly from 128 mAh g^{-1} to 116 mAh g^{-1}, retaining more than 90% of its original value. In addition, the columbic efficiency in both cases are greater than 99%. It has been proposed that dendrite growth on anode is a key factor limiting battery's lifetime [44,45]. The excellent cycling stability in the two tests suggest that dendrite growth should be insignificant in the PAEKNW-SPE batteries after 200 charge/discharge cycle. Variation in AC impedance spectra (cycle-1st cycle-50^{th} cycle-100^{th} cycle-200^{th} at 0.5C) of Li/PAEKNW-SPE/$LiFePO_4$ cells are shown in Fig. 6f. It can be seen that, the bulk resistance of the $LiFePO_4$/PAEKNW-SPE/Li cell remains relatively stable after 50, 100 and 200 cycles, always less than 70 Ω. SEM images of anodes in the two tests (Fig. 6g ~ i) verify this reasoning. As shown in Fig. 6h, the anode surface after 200 cycles at 0.5C is not significantly different from the surface of fresh lithium anode (Fig. 6g). Although there are some defects on the Li anode surface (Fig. 6i) after 200 cycles at 1C, no apparent lithium dendrites are observed. The results are also consistent with the symmetric cell measurements in Fig. 4.

4. Conclusion

A novel nonflammable Li-battery based on a unique hybridized solid-gel approach is developed, using an interpenetrating rigid-flexible poly (aryl ether ketone) nonwovens (PAEKNW) cross-linked with poly (ethylene glycol) dimethacrylate electrolyte to transport lithium ions, $LiFePO_4$ as cathode, and Li metal as anode. The battery works very well at room temperature and effectively suppresses the risks of burning or explosion. It does not readily catch fire or shrink, even under open flame, in stark contrast to most liquid-electrolytes-based batteries, and shows no noticeable volumetric expansion or contraction at 80 °C after 1h. Even after deliberately cut off one-third, the battery continues to function, with only a negligible drop in voltage (< 0.04V). The exceptional battery performances result largely from the unique bi-functional molecular design of the polymer electrolyte which guarantees simultaneously a very rare combination of thermal and mechanical stability, high ion conductivity, and a wide electrochemical window (> 4.5V) at room temperature. The design combines the advantages of both solid state and gel batteries but avoids many of their respective limitations. Although the molecular structure of the electrolyte system is sophisticated, the procedure to fabricate the electrolyte film is simple and straightforward, and can be easily scalable for industrial production. The cross-linked SPE forms a stable ESI on the surface of Li metal anode, which helps to suppress the Li dendrite and improves the cycling stability and long-term performance of the Li-metal batteries. The capacity reaches 124 mAh g^{-1} and 116 mAh g^{-1} after 200 cycles at 0.5C

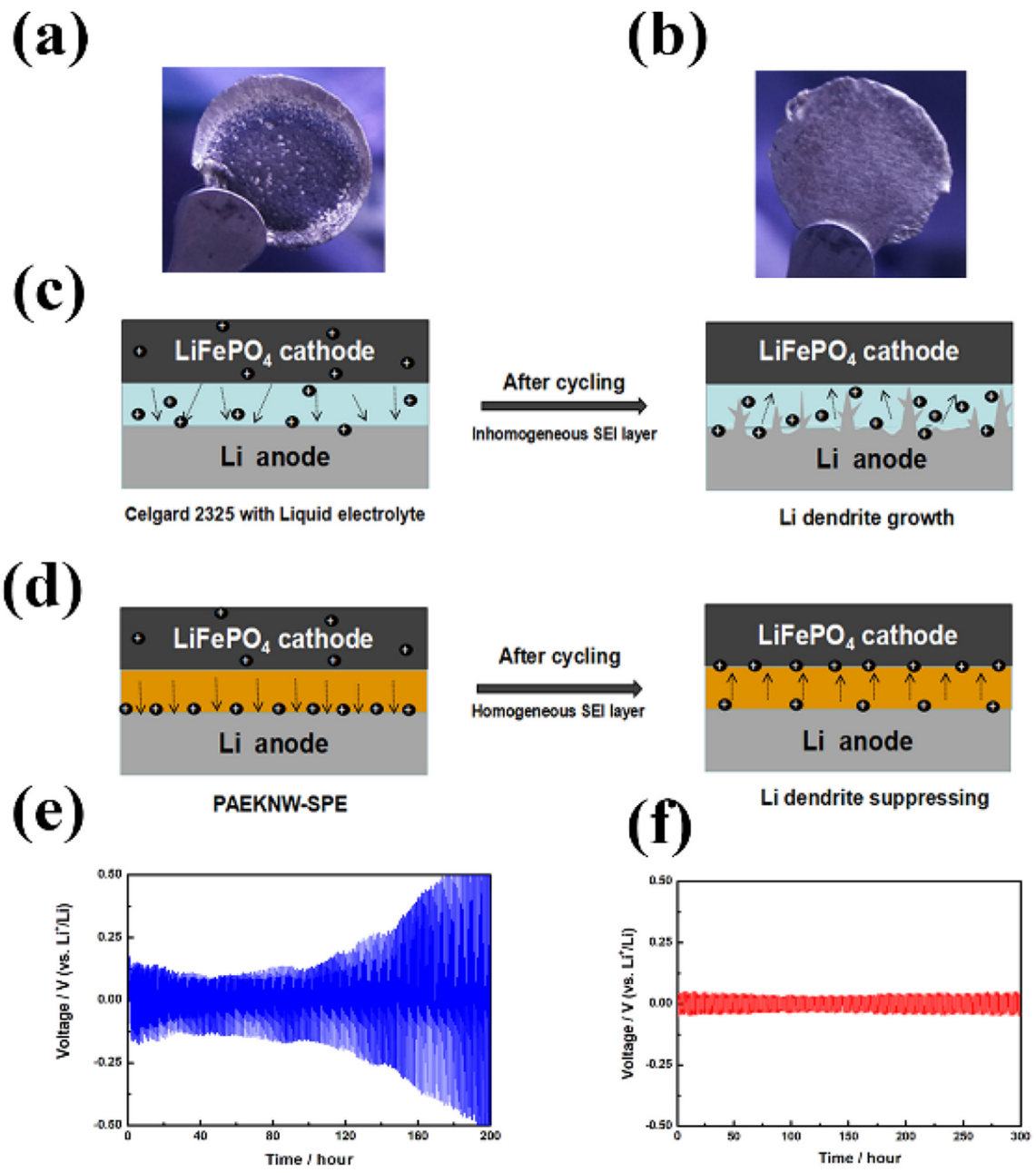

Fig. 4. Images of Li anode of batteries (a) with commercial liquid electrolyte and (b) with PAEKNW-SPE after 20 charge/discharge cycles. Li dendrites are clearly visible on the anode of liquid cell but barely exist on the anode of PAEKNW-SPE cell. (c) & (d) illustrations of SEI layers affected by dendrites. (e) & (f) Overpotentails of symmetric cells made from (e) liquid electrolyte and (f) PAEKNW-SPE at a current density of 1 mA cm^{-2} for 1 mA h.

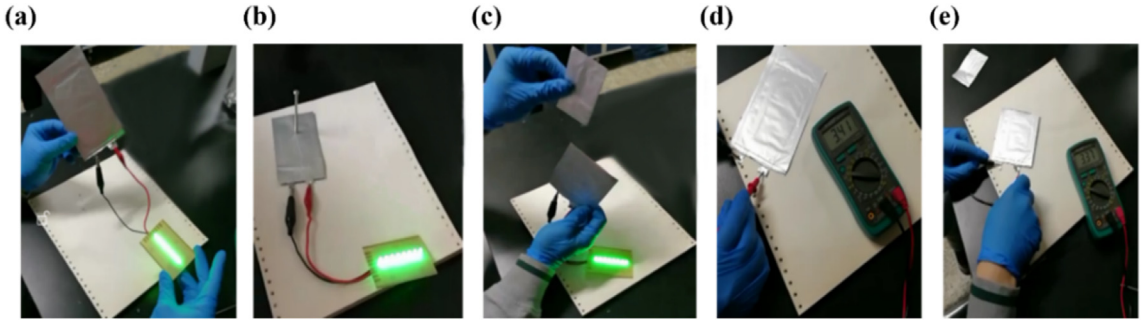

Fig. 5. (a) A soft package cell assembled with PAEKNW-SPE, which powers a group of LED lamps. (b) The cell remaining functional after nailed through. (c) The cell remaining functional after one-third is cut off. (d) and (e) the voltage of the cell only drop slightly from 3.41V to 3.37V, after one-third is cut off.

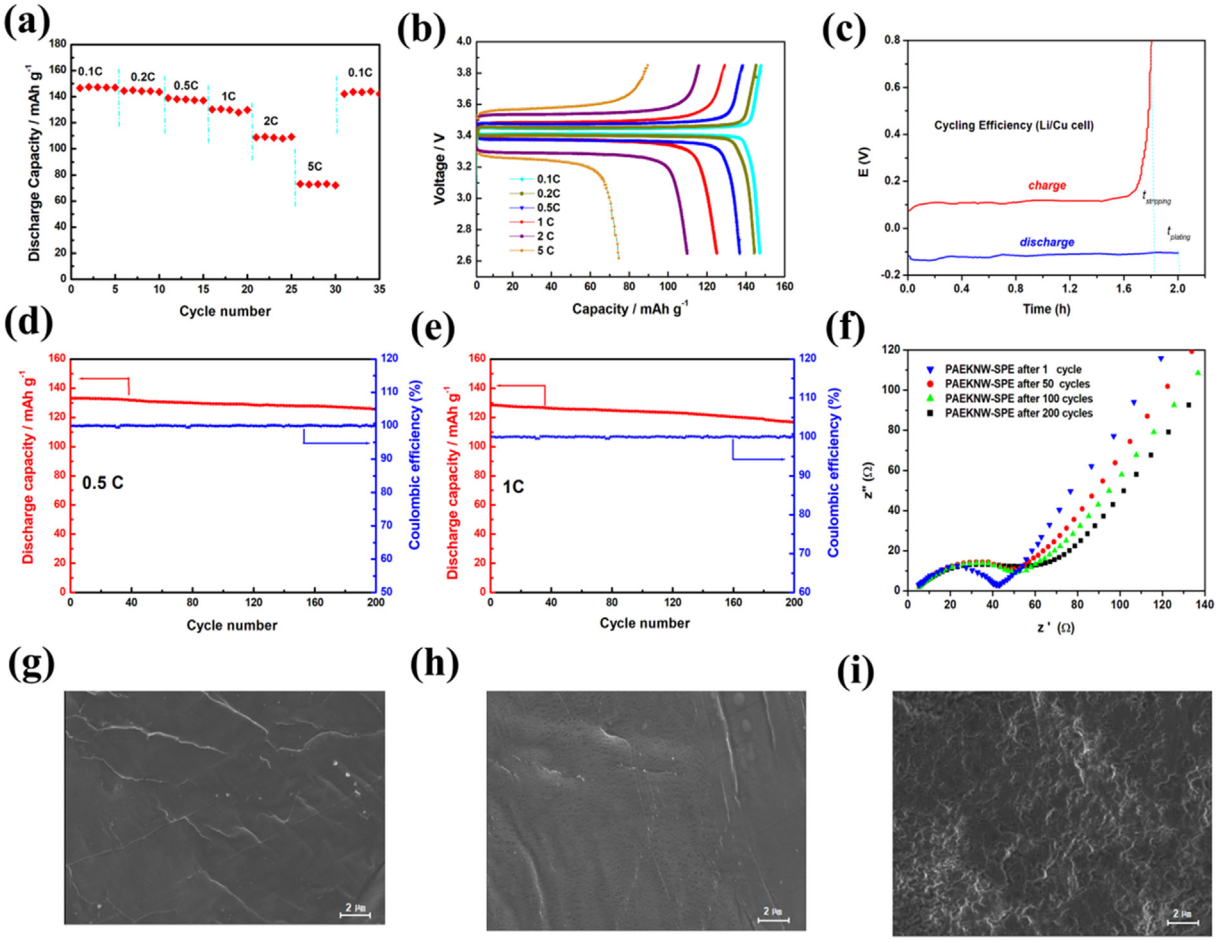

Fig. 6. (a) Battery capacities at different charge/discharge rates. (b) Galvanostatic charge/discharge profiles of first cycle at different rates. (c) Coulombic efficiency of Li plating/stripping test with Li/Cu cell. (d) and (e) Cycling performance and columbic efficiency of Li/PAEKNW-SPE/$LiFePO_4$ cells at 0.5C and 1C. (f) EIS of the $LiFePO_4$/PAEKNW-SPE/Li cells after 1, 50, 100 and 200 cycles at 0.5C. SEM images of the surface of Li electrode (g) before galvanostatic, (h) and (i) Li electrode obtained from a $LiFePO_4$/PAEKNW-SPE/Li cell after 200 cycles at 0.5C and 1C, respectively.

and 1C, respectively, both values are more than 90% percent of its corresponding initial values. The ease of processing and excellent comprehensive battery performances make the approach a very promising direction of safe lithium metal batteries.

Author contributions

GBL and JRZ designed experiments, GBL and LXM conducted experiments, GBL, XC, JTC, and JRZ wrote the paper, and JRZ supervised the project. All authors discussed and commented on the manuscript.

Acknowledgment

The work is supported by Fujian Minhua Power Source Co., Ltd and NSFC (NSFC-21627805, 21673004, 21673008) and MOST (2017YFA0204702) China. We also thank Drs. Jitian Liu and Chao Hou, and Ms. Limei Zhang's help.

Appendix A. Supplementary data

Supplementary data related to this article can be found at http://dx.doi.org/10.1016/j.jpowsour.2018.05.048.

References

[1] M. Armand, J.M. Tarason, Building better batteries, Nature 451 (2008) 652–657.
[2] G. Nystrom, A. Razaq, M. Stromme, L. Nyholm, A. Miharnyan, Ultrafast all-polymer paper-based, Nano Lett. 9 (2009) 3635–3639.
[3] J.B. Goodenough, Y. Kim, Challenges for rechargeable Li batteries, Chem. Mater. 22 (2010) 587–603.
[4] X. Wu, Z. Wang, X. Li, H. Guo, Y. Zhang, W. Xiao, Effect of lithium difluoro (oxalato) borate and heptamethyldisilazane with different concentrations on cycling performance of $LiMn_2O_4$, J. Power Sources 204 (2012) 133–138.
[5] W.D. Zhou, S.F. Wang, Y.T. Li, S. Xin, A. Manthiram, J.B. Goodenough, Plating a dendrite-free lithium anode with a polymer/ceramic/polymer sandwich electrolyte, J. Am. Chem. Soc. 138 (2016) 9385–9388.
[6] R. Kanno, M. Murayama, T. Inada, T. Kobayashi, K. Sakamoto, N. Sonoyama, A. Yamada, S. Kondo, A self-assembled breathing interface for all-solid-state ceramic lithium batteries, Electrochem. Solid State Lett. 7 (2004) A455–A458.
[7] R. Khurana, J.L. Schaefer, L.A. Archer, G.W. Coates, Suppression of lithium dendrite growth using cross-linked polyethylene/poly (ethylene oxide) electrolytes: a new approach for practical lithium-metal polymer batteries, J. Am. Chem. Soc. 136 (2014) 7395–7402.
[8] F. Croce, G.B. Appetecchi, L. Persi, B. Scrosati, Nanocomposite polymer electrolytes for lithium batteries, Nature 394 (1998) 456–458.
[9] N. Chen, Y.J. Dai, Y. Xing, L.L. Wang, C. Guo, R.J. Chen, S.J. Guo, F. Wu, Biomimetic ant-nest ionogel electrolyte boosts the performance of dendrite-free lithium batteries, Energy Environ. Sci. 10 (2017) 1660–1667.
[10] E. Quartarone, P. Mustarelli, Electrolyte for solid- state lithium rechargeable batteries:recent advances and perspectives, Chem. Soc. Rev. 40 (2011) 2525–2540.
[11] M. Nagao, H. Kitaura, A. Hayashi, M. Tatsumisago, High rate performance, wide temperature operation and long cyclability of all- solid-state rechargeable lithium batteries using Mo-S chevrel-phase compound, J. Electrochem. Soc. 160 (2013) A819–A823.
[12] K. Xu, Electrolytes and interphases in Li-ion batteries and beyond, Chem. Rev. 114 (2014) 11503–11618.
[13] N. Lago, O.G. Calvo, J.M.L. Amo, T. Rojo, M. Armand, All-solid-state lithium-ion batteries with grafted ceramic nanoparticles dispersed in solid polymer electrolytes, Chem. Sus. Chem. 8 (2015) 3039–3043.
[14] M. Kalita, M. Bukat, M. Ciosek, M. Siekierski, S.H. Chung, T. Rodriguez, S.G. Greenbaum, R. Kovarsky, D. Golodnitsky, E. Peled, D. Zane, B. Scrosati,

W. Wieczorek, Effect of calixpyrrole in PEO-$LiBF_4$ polymer electrolytes, Electrochim. Acta 50 (2005) 3942–3948.
[15] Y.F. Tong, L. Chen, X.H. He, Y.W. Chen, Free mesogen assisted assembly of the star-shaped liquid-crystalline copolymer/polyethylene oxide solid electrolytes for lithium ion batteries, Electrochim. Acta 118 (2014) 33–40.
[16] G.G. Zhou, F. Li, H.M. Cheng, Progress in flexible lithium batteries and future prospects, Energy Environ. Sci. 7 (2014) 1307–1338.
[17] J.J. Zhang, J.H. Zhao, L.P. Yue, Q.F. Wang, J.C. Chai, Z.H. Liu, X.H. Zhou, H. Li, Y.G. Guo, G.L. Cui, L.Q. Chen, Safety-Reinforced poly (propylene carbonate)-based all-solid-state polymer electrolyte for ambient-temperature solid polymer lithium batteries, Adv. Energy. Mater. 5 (2015) 1501082.
[18] Y. Wang, L. Zhang, L.Y. Zhang, F. Zhang, P. He, H.H. Zheng, H.S. Zhou, Reversible lithium-ion uptake in poly(methylmethacrylate) thin-film via lithiation/delithiation at in situ formed intramolecular cyclopentanedione, Adv. Energy. Mater. 6 (2016) 1601375.
[19] W. Xu, J.L. Wang, F. Ding, X.L. Chen, E. Nasybulin, Y.H. Zhang, J.G. Zhang, Lithium metal anodes for rechargeable batteries, Energy Environ. Sci. 7 (2014) 513–537.
[20] Z.Y. Lin, X.W. Guo, H.J. Yu, Amorphous modified silyl-terminated 3D polymer electrolyte for high-performance lithium metal battery, Nanomater. Energy 41 (2017) 646–653.
[21] K.H. Choi, S.J. Cho, S.H. Kim, Y.H. Kwon, J.Y. Kim, S.Y. Lee, Thin, deformable, and safety-reinforced plastic crystal polymer electrolytes for high-performance flexible lithium-ion batteries, Adv. Funct. Mater. 24 (2014) 44–52.
[22] X.B. Cheng, R. Zhang, C.Z. Zhao, F. Wei, J.G. Zhang, Q. Zhang, A review of solid electrolyte interphases on lithium metal anode, Adv. Sci. 3 (2016) 1500213.
[23] D.C. Lin, W. Liu, Y.Y. Liu, H.R. Lee, P.C. Hsu, K. Liu, Y. Cui, High ionic conductivity of composite solid polymer electrolyte via in situ synthesis of monodispersed SiO_2 nanospheres in poly(ethylene oxide), Nano Lett. 16 (2016) 459–465.
[24] A.M. Stephan, Review on gel polymer electrolytes for lithium batteries, Eur. Polym. J. 42 (2006) 21–42.
[25] L. Procarelli, M.A. Aboudzadeh, L. Rubatat, J.R. Nair, A.S. Shaplov, C. Gerbaldi, D. Mecerreyes, Single-ion triblock copolymer electrolytes based on poly (ethylene oxide) and methacrylic sulfonamide blocks for lithium metal batteries, J. Power Sources 364 (2017) 191–199.
[26] G.M. Zhou, F. Li, H.M. Cheng, Progress in flexible lithium batteries and future prospects, Energy Environ. Sci. 7 (2014) 1307–1338.
[27] B. Oh, W.I. Jung, D.W. Kim, H.W. Rhee, Preparation of UV curable gel polymer electrolytes and their electrochemical properties, Bull. Kor. Chem. Soc. 23 (2002) 683–687.
[28] Z.N. Zheng, X. Gao, Y.W. Luo, S.P. Zhu, Employing gradient copolymer to achieve gel polymer electrolytes with high ionic conductivity, Macromolecules 49 (2016) 2179–2188.
[29] N.W. Li, Y.X. Yin, J.Y. Li, C.H. Zhang, Y.G. Guo, Passivation of lithium metal anode via hybrid ionic liquid electrolyte toward stable Li plating/stripping, Adv. Sci. 4 (2017) 1600400.
[30] R.P. Doyle, X. Chen, M. Macrae, A. Srungavarapu, L.J. Smith, M. Gopinadhan, C.O. Osuji, S. Granados-Focil, Poly(ethyleneimine)-based polymer blends as single-ion lithium conductors, Macromolecules 47 (2014) 3401–3408.
[31] C.X. Guo, C.M. Li, Recent advances in soft materials to build and functionalize hard structures for electrochemical energy storage and in situ electrochemical molecular biosensing, Adv. Funct. Mater. 26 (2016) 8824–8853.
[32] D.M. Tigelaar, A.E. Palker, C.M. Jackson, K.M. Anderson, J. Wainright, R.F. Savinell, Synthesis and properties of novel proton-conducting aromatic poly (ether sulfone)s that contain triazine groups, Macromolecules 42 (2009) 1888–1896.
[33] Y.S. Ye, J.-H. Choi, K.I. Winey, Y.A. Elabd, Polymerized ionic liquid block and random copolymers: effect of weak microphase separation on ion transport, Macromolecules 45 (2012) 7027–7035.
[34] J.B. Goodenough, K.S. Park, The Li-ion rechargeable battery: a Perspective, J. Am. Chem. Soc. 135 (2013) 1167–1176.
[35] A.C. Luntz, J. Voss, K. Reuter, Interfacial challenges in solid-state Li ion batteries, J. Phys. Chem. Lett. 6 (2015) 4599–4604.
[36] X.L. Wu, Y.G. Guo, J. Su, J.W. Xiong, Y.L. Zhang, L.J. Wan, Carbon-nanotube-decorated nano-$LiFePO_4$ cathode material with superior high-rate and low temperature performances for lithium-ion batteries, Adv. Energy. Mater. 3 (2013) 1155–1160.
[37] G.B. Li, C.J. Zhao, X.F. Li, D. Qi, C. Liu, F.Z. Bu, H. Na, Novel side-chain-type sulfonated diphenyl-based poly (arylene ether sulfone)s with a hydrogen-bonded network as proton exchange membranes, Polym. Chem. 6 (2015) 5911–5920.
[38] J. Ni, C.J. Zhao, G. Zhang, Y. Zhang, J. Wang, W.J. Ma, Z.G. Liu, H. Na, Novel self-crosslinked poly(aryl ether sulfone) for high alkaline stable and fuel resistant alkaline anion exchange membranes, Chem. Commun. 47 (2011) 8943–8945.
[39] X.F. Lu, C. Wang, Y. Wei, One-dimensional composite nanomaterials: synthesis by electrospinning and their applications, Small 5 (2009) 2349–2370.
[40] J.R. Zheng, M.D. Fayer, Solute-solvent complex kinetics and thermodynamics probed by 2d-IR vibrational echo chemical exchange spectroscopy, J. Phys. Chem. B 112 (2008) 10221.
[41] B. Jiang, V. Ponnuchamy, Y.N. Shen, X.M. Yang, K.J. Yuan, V. Vetere, S. Mossa, I. Skarmoutsos, Y.F. Zhang, J.R. Zheng, The anion effect on Li^+ ion coordination structure in ethylene carbonate solutions, J. Phys. Chem. Lett. 7 (2016) 3554–3559.
[42] J.R. Zheng, M.D. Fayer, Hydrogen bond lifetimes and energetics for solute/solvent complexes studied with 2D-IR vibrational echo spectroscopy, J. Am. Chem. Soc. 129 (2007) 4328–4335.
[43] Y.X. Ren, M. Liu, T.S. Zhao, L. Zeng, M.C. Wu, An aprotic lithium/polyiodide semi-liquid battery with an ionic shield, J. Power Sources 342 (2017) 9–16.
[44] C.P. Yang, K. Fu, Y. Zhang, E. Hitz, L.B. Hu, Protected lithium-metal anodes in batteries: from liquid to solid, Adv. Mater. 29 (2017) 1701169.
[45] C.X. Guo, C.M. Li, Recent advances in soft materials to build and functionalize hard structures for electrochemical energy storage and in situ electrochemical molecular biosensing, Adv. Funct. Mater. 26 (2016) 8824–8853.
[46] J. Miao, M. Moyauchi, T.J. Simmons, J.S. Dordick, R.J. Linhardt, Electrospinning of nanomaterials and applications in electronic components and devices, J. Nanosci. Nanotechnol. 10 (2010) 5507–5519.
[47] X. Zhang, T. Liu, S.F. Zhang, X. Huang, B.Q. Xu, Y.H. Lin, B. Xu, L.L. Li, C.W. Nan, Y. Shen, Synergistic coupling between $Li_{6.75}La_3Zr_{1.75}Ta_{0.25}O_{12}$ and poly(vinylidene fluoride) induces high ionic conductivity, mechanical strength, and thermal stability of solid composite electrolytes, J. Am. Chem. Soc. 139 (39) (2017) 13779–13785.